

**Zeitschrift:** IABSE reports of the working commissions = Rapports des commissions de travail AIPC = IVBH Berichte der Arbeitskommissionen

**Band:** 33 (1981)

**Artikel:** Finite element modelling of reinforced concrete structures

**Autor:** Argyris, J.H. / Faust, G. / Willam, K.J.

**DOI:** <https://doi.org/10.5169/seals-26265>

### **Nutzungsbedingungen**

Die ETH-Bibliothek ist die Anbieterin der digitalisierten Zeitschriften auf E-Periodica. Sie besitzt keine Urheberrechte an den Zeitschriften und ist nicht verantwortlich für deren Inhalte. Die Rechte liegen in der Regel bei den Herausgebern beziehungsweise den externen Rechteinhabern. Das Veröffentlichen von Bildern in Print- und Online-Publikationen sowie auf Social Media-Kanälen oder Webseiten ist nur mit vorheriger Genehmigung der Rechteinhaber erlaubt. [Mehr erfahren](#)

### **Conditions d'utilisation**

L'ETH Library est le fournisseur des revues numérisées. Elle ne détient aucun droit d'auteur sur les revues et n'est pas responsable de leur contenu. En règle générale, les droits sont détenus par les éditeurs ou les détenteurs de droits externes. La reproduction d'images dans des publications imprimées ou en ligne ainsi que sur des canaux de médias sociaux ou des sites web n'est autorisée qu'avec l'accord préalable des détenteurs des droits. [En savoir plus](#)

### **Terms of use**

The ETH Library is the provider of the digitised journals. It does not own any copyrights to the journals and is not responsible for their content. The rights usually lie with the publishers or the external rights holders. Publishing images in print and online publications, as well as on social media channels or websites, is only permitted with the prior consent of the rights holders. [Find out more](#)

**Download PDF:** 29.03.2026

**ETH-Bibliothek Zürich, E-Periodica, <https://www.e-periodica.ch>**

## **Finite Element Modelling of Reinforced Concrete Structures**

Eléments finis pour le calcul de structures en béton armé

Finite Elemente zur Berechnung von Stahlbetontragwerken

**J.H. ARGYRIS**

Professor of Aeronautics

**G. FAUST**

Research Associate

**K.J. WILLAM**

Privatdozent

Institute of Statics and Dynamics for Aerospace Systems, University of Stuttgart  
Stuttgart, Fed. Rep. of Germany

### **SUMMARY**

The state of the art in finite element modelling of reinforced concrete structures is examined in three areas

- the spatial idealisation of composite structures,
- the constitutive models for the short-term behaviour of concrete under triaxial conditions, and
- the computational implications of rate type-constitutive formulations on the structural level

### **RESUME**

L'application de la méthode des éléments finis aux structures en béton armé est considérée sous trois aspects

- l'idéalisation spatiale des structures composites,
- les lois constitutives des matériaux pour le comportement tridimensionnel,
- les questions de calculs des structures pour un comportement inélastique des matériaux

### **ZUSAMMENFASSUNG**

Der Beitrag beschäftigt sich mit der Finiten Element Methode und ihrer Anwendung im Stahlbetonbau. Drei Themen werden untersucht,

- die räumliche Idealisierung des Verbundwerkstoffes,
- die Formulierung von Stoffgesetzen für das Kurzzeitverhalten im dreiaxialen Bereich, und
- die rechentechnischen Fragen bei der Behandlung von inelastischen Werkstoffvorgängen auf der Tragwerksebene



## 1. INTRODUCTION

Modern computational techniques and, in particular, the finite element method have been used in nonlinear analysis of reinforced concrete structures for more than a decade [1], [2], [3], [4]. In spite of intensive research activities on the refinement of reinforced concrete models there are still several open questions, partly also because they have never been posed before the advent of computers in structural mechanics. Another source of discomfort are the difficulties in the prediction of the ultimate load behaviour of such simple structures as deep and over-reinforced beams. In contradistinction to simple limit analysis concepts of beams we recognise that two- and three-dimensional finite element idealisations trace the entire history of structural degradation starting from tensile cracking to the nonlinear deformation behaviour in compression up to crushing and debonding and other interactive effects between concrete and reinforcement. Therefore, the finite element model is today primarily a tool for interpreting experimental observations and for studying constitutive assumptions and their effects on the overall performance of the structure rather than a new method for standard design problems. Clearly, nonlinear solutions are very costly, especially if two- or three-dimensional idealisations are used and, in particular, if the limit load behaviour is of primary concern. In this case the integrity or rather the stability of the structure has to be assessed at increasing load levels whereby the overall nonlinear response behaviour is approximated by a series of linearised steps.

The long-term serviceability is normally assessed in the linear regime. Implicitly it is assumed that the dead and life loads are sufficiently small so that the nonlinearity in the elastic and inelastic deformations can be neglected. This is necessary for long-term creep predictions with the effective modulus methods, however, it is no prerequisite for step-by-step time marching strategies in which cracking and other nonlinear concrete effects are traced with the appropriate time-operators. This approach lends itself also to the finite element solution of environmental transients which can be readily combined with the time dependent inelastic analysis of structures. In this case the partitioned solution scheme leads to a staggered computational path in which the thermal and hygral effects are normally introduced into the equation of motion in the form of thermal expansion and shrinkage (one-way thermomechanical and hygrothermal coupling).

At this stage it might be worthwhile to reflect upon the underlying postulates for the finite element modelling of reinforced concrete structures. Clearly, the combined effect of spatial idealisation, constitutive assumption and computational path is critical for the predictive value of the final solution. In the following, these three aspects will be discussed and assessed in the light of recent finite element developments. The lack of agreement among leading researchers in this context is an indication that there is still a need for a better understanding of the mechanics of reinforced concrete structures and its characterisation in a computer-oriented solution environment. Certainly, there is some justification for self-criticism of the complexity and cost of extensive finite element studies, however, this computer-oriented method gives us a chance to project constitutive observations onto the structural level and to examine their effects on the overall response of the structure.

## 2. STRUCTURAL IDEALISATION

The finite element method is most successful when we are dealing with composite structures. The heterogeneity can be readily modelled with separate elements including special elements for the interface conditions.

The spatial idealisation of reinforced concrete structures requires homogenisation at various levels:

- (i) the configuration of the composite and
- (ii) the fracture response at localised failure.

In the following, these two aspects are briefly examined together with a discussion of modelling aspects of reinforced concrete frames, plates and shells.

## 2.1 Modelling of the composite material

On the microscale the heterogeneous composition of concrete, the cement stone, aggregate and adhesive bonding is modelled with the same ease as the composite action of concrete, steel reinforcement and their various interaction mechanisms on the macroscale. On an even larger scale, the composite may be homogenised entirely and described by equivalent isotropic or anisotropic material properties. This latter approach is certainly suitable for fibre-reinforced concrete, however, for the usual reinforced concrete structures this averaging technique is only appropriate if the global behaviour of the structure is of interest in the working stress regime. Clearly, tensile cracking and other specific concrete phenomena can be considered in this case only by the corresponding degradation of the "equivalent" material properties. This indicates the basic shortcoming of homogenisation which can only account for the combined response behaviour in the form of an average.

In reinforced concrete the large difference of concrete and steel behaviour is normally accounted for by a discrete approach where the configuration and mechanical behaviour of each constituent is modelled individually by appropriate finite elements. Perfect bond is usually assumed in order to reduce the number of degrees of freedom and to avoid the inherent difficulties in assigning appropriate bond properties. In this way, the complex interaction problem is circumvented, however pull-out effects as well as tension stiffening, dowel action and spalling cannot be accounted for directly except by "corresponding" modifications of the stiffness and strength properties of the constituents.

## 2.2 Modelling of the fracture process

Another major problem arises at the ultimate load analysis of reinforced concrete components. Here progressive cracking and gradual damage accumulation leads eventually to the localisation of discrete failure zones. The numerical modelling of the entire response spectrum is one of the open problems in the finite element analysis of reinforced concrete components. There are basically two approaches for the spatial idealisation of cracking, damage and localised fracture, the

- smeared crack model, and the
- discrete crack model.

Computationally the smearing approach is far more convenient since the topology of the idealised structure remains intact and all local discontinuities due to cracking, fracture and localised damage are distributed evenly over the element domain. This averaging procedure fits the scope of continuum mechanics or rather strength of material and the nature of the finite element displacement method where continuity of the displacement field and boundedness of the stress field are inherent properties.



In contrast, the discrete crack approach poses complex computational problems since the topology and the finite element mesh changes with the history of crack propagation. Traditionally, the question of fracture initiation and fracture propagation is here dealt with within strength of material concepts in which e.g. tensile cracking is defined in terms of maximum stress or strain. In this case, the entire fracture model depends primarily on the spatial idealisation and thus fracture is a question of mesh refinement rather than one of an objective measure of stress intensity or damage per unit volume. Therefore, recent attempts are directed towards the development of fracture mechanics concepts for the failure prediction of concrete. The main difficulty is here that linear fracture mechanics provides only a statement of stability or rather catastrophic failure of a given crack, while slow crack propagation necessitates additional concepts such as blunting, localized plastification at the crack tip and also large deformations. Here the  $\int$ -integral and alternative energy criteria are rather promising candidates since they are combined measures of stress and strain. It is intriguing that such models also account for gradient effects as long as they are referred to a unit volume which has e.g. the size of the aggregate. These latter concept requires however further studies and is the subject of current research activities.

### 2.3 Modelling of flexural components

A particularly difficult modelling task is the finite element idealisation of flexural components where the dimensionality of the structural configuration is normally reduced by one with the aid of the Kirchhoff hypothesis. The development of consistent beam, plate and shell elements is however by no means trivial even for the simple case of linear elastic behaviour and a homogeneous cross-section. The Kirchhoff kinematics complicates unduly the construction of sound displacement models which maintain the convergence requirements as well as full compatibility before and after deformation. This is particularly true for curved shell elements but also for flat elements where the different order of expansion for membrane and bending action is often a source of serious discomfort. Alternatively, these kinematic difficulties are avoided by mixed and hybrid models or so-called degenerate solid elements which do not enforce the Kirchhoff kinematics and allow for shear deformations. These so-called degenerate solid elements lead to an excessive number of degrees of freedom if cubic expansions are used. Therefore, selective integration is used in order to capture the bending behaviour with a lower expansion and a smaller number of degrees of freedom. This corresponds to a decomposition of the strain energy into different components and a balancing of membrane, bending and transverse shear contributions by reduced integration.

For nonlinear and inelastic material behaviour the situation becomes even more complex. In this case the integration over the thickness has to be carried out by numerical integration which corresponds in the case of piecewise constant approximations to the familiar layering of the cross-section. Clearly, the data volume and the computational effort for evaluating the element properties increases proportionally with the number of layers but the total number of structural degrees of freedom remains constant. There are various proposals to by-pass the layered idealisation of bending problems e.g. by using stress resultants (first and higher order moments) and the corresponding integral formulation of the material law. All these homogenisations through the thickness suffer from severe shortcoming of a continuous stress distribution over the thickness which excludes non-monotonic and non-proportional loading paths in elasto-plasticity (restriction to the deformation theory of plasticity). Moreover, the interaction of inelastic membrane and bending behaviour can be properly incorporated only for cases when the two sets of principal axes coincide while transverse shear effects are neglected altogether. This transverse shear is also problematic in the layered approach because it exceeds the plane stress formulation adopted in the Kirchhoff models. The degenerate

solid elements offer some resolution since they can resort to a full three-dimensional material law. On the other hand the selective integration introduces here another complication since the individual contributions to the strain energy are evaluated at different pivot points.

In summary, the modelling of frame, plate and shell elements is rather complex due to the peculiar behaviour of reinforced concrete. The layered approach is however sufficiently general although debonding and shear failure have to be excluded if we adhere to the Kirchhoff kinematics. For this reason the notion of a pure displacement model is normally given up and equilibrium considerations are invoked in order to incorporate transverse shear effects in a global fashion and to account for tension stiffening because of finite crack spacing.

### 3. CONSTITUTIVE MODELS

The finite element analysis of reinforced concrete structures is restricted primarily by the shortcomings of the underlying constitutive models. Although the spatial idealisation can be refined to capture every detail of the structural configuration within the scope of sophisticated two- and three-dimensional finite element packages, the material characterisation of the concrete and the interface conditions is rather limited. As a matter of fact, rather simple constitutive postulates are normally adopted for the strength and the deformation behaviour under biaxial and triaxial conditions. For ultimate load studies these assumptions must cover the entire loading regime because the post-failure range is often crucial for the overall reserve strength and the redistribution capacity of indeterminate structures. This stress transfer introduces locally non-proportional loading paths with extensive unloading regimes although the external loading is still increasing monotonically. The material degradation due to progressive damage leads finally to localised fracture in which high gradients mobilise additional strength reserves beyond the data which are normally obtained from uniform stress specimens. The influence of different loading rates is usually neglected for short-term loadings, however in dynamic environments and quasistatic creep problems it dominates the response behaviour and must be included. The ultimate failure behaviour of reinforced concrete composites depends to a large extent on the interface properties between concrete and steel. Clearly, under extreme loading conditions these effects become very important and affect the overall performance of the composite structure.

In the following, two aspects of the mechanical behaviour are considered, the strength and the deformation characteristics of concrete when subjected to uniaxial and multiaxial loadings. Historically, the bulk of experimental work was and still is directed towards the response in uniaxial compression, while the other facets of the mechanical behaviour are expressed in terms of this fundamental property. Because of the experimental difficulties, multiaxial testing was primarily concerned with the evaluation of the strength properties. Only recently have deformation data become available for test set-ups which are truly triaxial [5]. Therefore, the failure models are in general more advanced than the corresponding nonlinear deformation models in the pre- and post-failure regime. In some cases strength and deformation behaviour are considered to be entirely independent properties while other models such as hypoelastic and endochronic formulations contain no explicit strength statements whatsoever. At this stage it is worthwhile to scrutinise some established constitutive concepts for the multiaxial behaviour of concrete under short-term loading in the light of the recent results from the international testing program [5].



### 3.1 Strength models

We consider here the general case of triaxial concrete strength which should cover also the biaxial and uniaxial cases. The numerous papers on the subject indicate however that the generalisation of the uniaxial strength values to triaxial conditions is by no means a trivial task.

There are two basic postulates which are normally adopted in order to simplify the construction of triaxial failure conditions

- isotropy, and
- convexity in principal stress space.

The first assumption is introduced because of the triple-symmetry in the triaxial stress space and the inherent simplification of the failure model. In reality, progressive damage leads certainly to oriented anisotropies near ultimate behaviour which require however the formulation of failure conditions in the six-dimensional stress space instead of the three-dimensional space of principal stresses. Because of the inherent complexity and the lack of experimental evidence it is reasonable to assume "isotropic" behaviour up to failure and even thereafter in the post-failure regime.

Clearly, the maximum shear strength increases with hydrostatic compression and exhibits a pronounced dependence on the third stress invariant (synonymous to the direction in the deviatoric plane). In summary, it is widely accepted that the failure condition is a function of all three stress invariants [6], [7] and that it is poorly reproduced by the axisymmetric Drucker-Prager cone or paraboloid formulated originally by Schleicher.

Convexity is an assumption which is supported by global stability arguments in plasticity. Clearly, there are some questions on the validity of this postulate for concrete, particularly if local material instabilities are considered in the post-failure regime. For the initial failure surface however convexity in the principal stress space is generally accepted even though it does not necessarily imply convexity in the six-dimensional stress space because of the non-quadratic form of the third invariant. It is intriguing that an alternative representation in the strain space may also introduce non-convex surfaces in spite of a convex strength model in stress space. In principle, a strain representation of failure has computational advantages if we think of finite element displacement models and material stability studies. However, the failure condition in strain space is certainly far more irregular than in stress space.

There are two basic groups of failure models depending on the smoothness of the failure surface. The first class with discontinuous curvatures follows essentially the traditional Mohr-Coulomb criterion with tension cut-off [8], [9]. The second class rests on the concept of an extended Drucker-Prager model which includes the effect of the third stress invariant [10], [11]. From a numerical standpoint the discontinuities complicate the analysis since the failure surface has to be divided into subregions and due to difficulties of defining a unique stress transfer path at the corners. On the other hand, the discontinuous failure description furnishes additional information on the type of failure (tensile-cracking or shear sliding) and the direction of failure. In contrast the continuous descriptions can not provide statements of this sort if no additional concepts such as normality are invoked.

A recent comparison of the triaxial test data of the international program indicates that the continuously curved strength models with all three stress invariants yield a close overall approximation of the experimental results [12]. The Fig. 1 illustrates the construction of the



five parameter model by the authors [10] which is made up of an elliptic approximation of the deviatoric trace and a parabolic description in the Rendulic plane. Fig. 2 shows the triaxial strength data of the BAM [7] in comparison to the hydrostatic prediction of the five parameter model using the least square values of [12]. The corresponding deviatoric results are displayed in Fig. 3 for  $\bar{\sigma}_\alpha = -1.25 f_c$ . Fig. 4 shows the trace in the biaxial plane  $\bar{\sigma}_1 = 0$  which is the most severe test of the triaxial failure model because of the large magnification of approximation errors due to the very acute angle of intersection. The plots indicate satisfactory agreement whereby the strength ratios  $\alpha_2 = f_t / f_c$  and  $\alpha_u = f_b / f_c$  are fixed from the biaxial concrete data. Thus the deviatoric radial vectors  $f_1, f_2$  at a given section  $\bar{\sigma}_\alpha = -\xi$  are the only free optimisation variables for fitting specific triaxial strength data.

The failure surface in stress space is certainly a first step towards defining the concrete behaviour under triaxial conditions. Clearly, we have to pose additional questions such as - what happens to the failure surface when the loading path reaches this strength constraint? In one limiting case of ideally plastic behaviour, the failure surface remains fixed in stress space while in the other limiting condition of ideally brittle behaviour it collapses suddenly to another configuration of residual strength. The actual post-failure behaviour in compression but also in tension lies certainly somewhere in between these two extremes (continuous softening in kinematically constrained specimens). On the other hand, the material already degrades progressively in compression before the limiting strength is reached. Therefore, if we consider hardening the failure model can be also utilised to define the nonlinearity in the pre-failure regime. This leads us to the general question of nonlinear deformation behaviour in the pre- and post-failure regime (hardening-softening models for triaxial conditions) and its representation for triaxial conditions.

### 3.2 Nonlinear deformation models

Two classes of constitutive models can be distinguished

- (i) algebraic stress-strain laws based on a total (finite) formulation, and
- (ii) differential stress-strain laws based on an incremental (infinitesimal) formulation.

The first class involves invariably nonlinear algebraic equations (secant laws) which arise e.g. in nonlinear elasticity (hyperelasticity) and the deformation theory of plasticity. The main advantages of this secant stiffness formulation are primarily numerical such as the full error control via unbalanced load iteration (no drift) and the unproblematic treatment of softening. The principal disadvantages are well-known, the total stress-strain laws restrict the range of application to primarily monotonic loading regimes. This limitation is rather severe since there are only very few actual problems without local unloading due to stress redistribution and with a frozen pattern of principal axes. In praxis, however, these effects are disregarded and many developments for the ultimate load analysis of statically undetermined problems resort to the total form of the stress-strain law because of its simplicity.

The differential rate models involve invariably tangential stress-strain laws which arise typically in hypoelasticity, plasticity, endochronic theory or alternative inelastic evolution laws. The main advantages of this tangential stiffness formulation are linearity (the tangential material law normally depends on the state variables - stress, strain etc. - but not on their differentials) and the broad range of application to non-monotonic, non-proportional loading regimes. In contrast to hypoelastic and endochronic models a proper loading condition is introduced in the flow theory of plasticity which separates elastic from inelastic behaviour. Therefore, nonlinearity and damage are mobilised only if a certain stress-threshold (the yield



condition) is exceeded while no damage can accumulate below that value. Furthermore, normality and convexity guarantee a stable material law in accordance with the dissipation inequality which is violated by variable moduli techniques in which a loading concept is introduced arbitrarily in order to distinguish loading and unloading branches [13]. It should be noted that a pure rate formulation does not result by mere differentiation of the secant moduli in the total formulation of the stress-strain law [14].

The principal disadvantages of the rate models are well-known, they are primarily numerical since they require step by step integration. The accumulation of the linearisation errors might lead to a considerable drift if truly finite increments are used for advancing the tangential approach and if a refined error control is lacking. Moreover, the tracing of softening branches is complicated by local singularities at the limiting points for which geometric stiffness effects might be important and should be included.

Broadly speaking there are three families of constitutive relationships according to the underlying theory of nonlinear elasticity, elasto-plasticity and endochronic or internal variable theory, respectively. In spite of a centennium of concrete technology there is still no single constitutive model which covers all facets of the mechanical behaviour of concrete. Therefore, we must be satisfied at this stage with phenomenological models which reproduce specific aspects of the response behaviour without violating fundamental principles of mechanics. Clearly, the modelling itself is an underdetermined problem because of the inherent non-linearity and even more so because of the history dependence. This latter property alters the scope of the formulation from a relatively "simple" description of nonlinear equilibrium states (algebraic approach) to the far more demanding characterisation of an evolutionary process (differential approach).

#### (i) Nonlinear elasticity models

This family of constitutive models describes the nonlinear deformation behaviour irrespectively of path-dependence. Their application is primarily directed towards monotonic loading regimes where no distinction must be made between loading and unloading behaviour. A priori, there is no limitation as far as proportional loading is concerned as long as an objective formulation is used which assures invariance with regard to coordinate transformations. The orthotropic models [15], [16], [17], [18] however assign different material properties to each principal direction, which should therefore remain fixed during the entire loading history if not a co-rotational definition of stress rate is used such as the Jaumann stress rate.

The principal task of constructing a nonlinear deformation model for multiaxial conditions can be recognised best from the uniaxial compression behaviour shown in Fig. 5. The hardening branch is fully defined by the initial modulus of elasticity  $E_0$  and the maximum strength  $\sigma_c$  where the tangent modulus approaches zero,  $E_T = 0$ . The associated strain  $\varepsilon_c$  defines the ductility when the maximum stress is reached. This tells us immediately that for a three-dimensional extension of the uniaxial law there is additional information required on the triaxial failure strain beyond the strength values discussed before. An alternative formulation resorts to the secant modulus  $E_s = \sigma_c / \varepsilon_c$  at triaxial failure which is however only another statement of the failure strain  $\varepsilon_c$  which is normally very strongly path-dependent. As a result, there is no simple approach for constructing a nonlinear deformation model which should start initially with the linear elastic properties and should then introduce progressive damaging up to singular behaviour of the tangential material law at the maximum strength value. If we proceed further into the softening regime, and this is of utmost importance for the evaluation of the reserve strength, we have to define an additional rupture strain  $\varepsilon_r$  and possibly also a reserve strength  $\sigma_r$ . For general triaxial conditions this property is very

difficult to define, thus ideal plasticity is often assumed up to a maximum rupture strain  $\epsilon_r$ , where full strength degradation takes place,  $\bar{\sigma}_r = 0$ .

There have been several proposals of the tangential material law; most noteworthy are the developments of a nonlinear secant formulation [19] for  $E_s$  and  $\nu_s$  introducing a non-linearity index as a scalar measure of "equivalent" triaxial stress. A very recent proposal [18] adopts the concept of the equivalent orthotropic strain in [17] in order to construct an incremental orthotropic material law with the aid of the five parameter strength model. The orthotropic properties are however somewhat in conflict with the usual definition of hypo-elasticity which exhibits stress induced anisotropy [20] but not orthotropic tangent moduli with reference to principal directions limiting the range of application of proportional loading if not a so-called objective stress rate is used.

In contradistinction to the engineering models above there are some developments which follow the classical concepts of hyper- and hypoelasticity. It is intriguing that there are no attempts to describe the nonlinear deformation behaviour of concrete in terms of a strain energy function  $U = U(\epsilon)$  where the total stress-strain law

$$\sigma = \frac{\partial U}{\partial \epsilon} \tag{3.1}$$

corresponds to the secant relationship

$$\sigma = E_s \epsilon \quad \text{with} \quad E_s = \frac{\partial U}{\partial \epsilon} \epsilon^{-1} \tag{3.2}$$

The associated rate law derives by differentiation of (3.1)

$$\dot{\sigma} = E_T \dot{\epsilon} \quad \text{with} \quad E_T = \frac{\partial^2 U}{\partial \epsilon \partial \epsilon^t} \tag{3.3}$$

Clearly, a quadratic power expansion of  $U(\epsilon)$  corresponds to linear stress-strain behaviour with  $E_T = \text{const}$ . Thus a fourth order strain energy function would be required in order to obtain a rate formulation (3.3) of grade two. For isotropic conditions the strain energy can be expressed in terms of the strain invariants  $U(\epsilon) = U(I_1, I_2, I_3)$ , however a fourth order expansion still involves 9 material constants whose identification poses certainly a formidable problem.

Traditionally, this task is simplified by decomposing the strain energy into hydrostatic and deviatoric components. As long as interaction effects remain negligible, which is certainly true for metals, the response due to hydrostatic stresses is purely hydrostatic and that due to deviatoric stresses purely deviatoric. Therefore, the strain energy decomposes into

$$U(\epsilon) = U_v(I_1) + U_d(I_2', I_3') \tag{3.4}$$

In [21] it was shown that the deviatoric component  $U_d$  cannot depend on the third invariant  $I_3'$  of deviatoric strains, thus  $U_d = U_d(I_2')$ . As a result, the modelling of nonlinear elastic deformation reduces to the evaluation of two single functions which describe the nonlinear volumetric and deviatoric behaviour



$$\sigma_v = 3 K_s (J_1) \epsilon_v \quad (3.5)$$

and

$$\sigma_d = 2 G_s (J_2') \epsilon_d \quad (3.6)$$

In [22] the  $K$  and  $G$  -approach was expressed in terms of the octahedral stress and strain components and applied successfully to interpret biaxial and recently also triaxial concrete data [23]. It was however noted that under truly triaxial conditions there is noticeable coupling between the hydrostatic response and the deviatoric loading. Therefore, the decomposition of  $u = u_v(J_1) + u_d(J_2')$  is debatable and some form of coupling has to be introduced, see e.g. [24].

It is intriguing that the incremental  $K$ - $G$  formulation is made up of two components and cannot be simplified to an expression involving only the tangent moduli [14] since differentiation of (3.6) yields

$$d\sigma_d = 2 \left( \epsilon_d \frac{dG_s}{dJ_2'} dJ_2' + G_s d\epsilon_d \right) \quad (3.7)$$

where  $\frac{dG_s}{dJ_2'} dJ_2' = \frac{3}{2} \frac{G_T - G_s}{J_2'} \epsilon_d^t d\epsilon_d$  and  $G_T = G_s + J_2' \frac{dG_s}{dJ_2'}$  (3.8)

The resulting tangential material law is therefore identical with the equivalent elastoplastic hardening von Mises formulation if  $K_T = \text{const}$  and monotonic loading is considered only.

This leads us to the direct formulation of a differential material law within the theory of hypoelasticity where

$$\dot{\sigma} = E_T \dot{\epsilon} \quad E_T = E_T(\sigma, \epsilon) \quad (3.9)$$

In the concrete literature the only attempt [20] develops an incremental constitutive law of grade one (linear in stress). Higher order expansions are forbidding because of the large number of material parameters although hypoelasticity is restricted a priori to isotropic conditions. In this context it is intriguing that the associated failure criterion can be identified with singularities of the tangential material law when  $\det E_T = 0$ .

## (ii) Plasticity models

Since most of the early finite element work on physical nonlinearities was directed towards elastoplastic computations it was natural to adopt hardening plasticity formulations for the nonlinear deformation behaviour of concrete in compression.

In contrast to the hypoelastic rate formulation the flow theory of plasticity accounts for path-dependence via the loading criterion. The inherent postulate of linear elastic unloading is certainly a first improvement when compared with the purely elastic formulation, however the lack of an elastic hysteresis for repeated unloading-reloading conditions exhibits



also shortcomings when compared with the experimental evidence in [25] (the endochronic and rate dependent viscoplastic formulations offer here some improvement).

In plasticity theory the difficulties with the identification of the tangent moduli in (3.9) are avoided altogether by resorting to the concept of a flow rule which controls the evolution of the inelastic deformation  $\dot{\eta}$  in terms of the yield surface  $f(\boldsymbol{\sigma}, \boldsymbol{\alpha}) = 0$

$$\dot{\eta} = \dot{\lambda} \frac{\partial f}{\partial \boldsymbol{\sigma}} \quad \text{with} \quad \dot{\eta} = \dot{\lambda} \left( \frac{\partial f}{\partial \boldsymbol{\sigma}} + \frac{\partial f}{\partial \boldsymbol{\alpha}} \right) \quad (3.10)$$

$\boldsymbol{\alpha}$  denote e.g. the current values of the five parameter yield surface in [10], [27]. The associated hardening rule determines the rate of change of the current yield surface and the normality condition  $\frac{\partial f}{\partial \boldsymbol{\sigma}}$  the direction of inelastic strain rate  $\dot{\eta}$ .

The first finite element applications to concrete in compression resorted to the well-established concepts of the Huber-Mises theory disregarding hardening due to volumetric compression. In this case a single hardening function suffices to describe the nonlinear deviatoric action in terms of the von Mises equivalent stress-strain diagram. This is equivalent to the tangential shear modulus of the nonlinear elastic  $K$ - $G$  formulation above, where  $K_T = \text{const}$ .

In order to include hydrostatic effects, the Drucker-Prager extension of the von Mises model was adopted in [26] whereby two intersecting conical yield surfaces were necessary in order to obtain satisfactory agreement with the triaxial failure surface in tension and compression. There is no longer a unique hardening function which covers the entire loading regime. As a matter of fact, the same disturbing observation was made by the authors in [27] where the five parameter model was adopted to describe hardening by an affine expansion of all parameters and softening by a translatory shift along the hydrostatic axis. The range of motion is shaded in Fig. 6 while Fig. 7 illustrates the corresponding hardening in uniaxial and biaxial compression.

In a recent publication [28] a three-parameter elasto-plastic strainhardening theory was presented for biaxial conditions in which the equivalent plastic strain rate was decomposed into two tensile and one compressive plastic strain parameters. Extending this approach to tri-axial conditions the current configuration of the five parameter model [10] is now defined by 5 independent hardening functions  $\alpha_1, \dots, \alpha_5$  in terms of the inelastic work  $A_i = \int \boldsymbol{\sigma} \dot{\eta}$  or the inelastic strain measure  $\bar{\eta} = \int (\dot{\eta}^t \dot{\eta})^{1/2}$ . To this end the increment of equivalent plastic strain  $\dot{\eta}$  is decomposed into the five plastic strains  $\eta_1, \dots, \eta_5$  by the mapping

$$\dot{\eta}_i = \beta_i \dot{\eta} \quad \text{with} \quad \sum_i \beta_i = 1 \quad (3.11)$$

The decomposition factors  $\beta_i$  define the participation of each plastic strain  $\eta_i$  in the overall hardening-softening whereby the sum of increments equals the increment of equivalent plastic strain increment  $\dot{\eta}$ . The individual hardening rules for each parameter  $\alpha_i$  of the five parameter yield surface are now



$$\begin{aligned}
 \alpha_1: \quad f_t &= f_t^0 + g_1(\eta_1) & - \text{uniaxial tension} \\
 \alpha_2: \quad f_c &= f_c^0 + g_2(\eta_2) & - \text{uniaxial compression} \\
 \alpha_3: \quad f_b &= f_b^0 + g_3(\eta_3) & - \text{biaxial compression} \\
 \alpha_4: \quad g_1 &= g_1^0 + g_4(\eta_4) & - \text{tensile shear at } \bar{\sigma}_a = -\xi \\
 \alpha_5: \quad g_2 &= g_2^0 + g_5(\eta_5) & - \text{compressive shear at } \bar{\sigma}_a = -\xi
 \end{aligned}$$

The hardening functions  $g_i(\eta_i)$  define the motion of the current yield surface in terms of the plastic strain values  $\eta_i$  and thus the equivalent plastic strain  $\bar{\eta}$ . For an assumed distribution of participation factors  $\beta_i$  the hardening functions  $g_i(\eta_i)$  must be identified from triaxial test data. Clearly, this is not a trivial task, also because the resulting yield surface must satisfy certain convexity requirements. Certainly in the simplest case of an affine expansion of the yield surface the current strength parameters  $\alpha_i$  must have the same normalised value which would correspond to the isotropic hardening plot in Fig. 6.

The formation of the ensuing differential material law follows the usual concepts of hardening plasticity, see e.g. [27], whereby the evaluation of the consistency rule  $\dot{\Phi}_i = 0$  for determining  $\dot{\eta}$  involves now differentials with regard to the five strain hardening parameters  $\alpha_1, \dots, \alpha_5$ .

In completion we should note the intriguing development of endochronic time models which provide a very accurate description of the nonlinear concrete behaviour [29]. Since no proper justice can be done to this topic in this context we only recall that there is little difference between plasticity and endochronic theory when a loading condition is introduced [30] except for the formulation in total strain space and the intricate mappings relating total strain with endochronic time. Without the unloading condition the endochronic model predicts continuous damage accumulation even at very low stress levels which has been criticised particularly for dynamic applications [31]. An interesting alternative to the endochronic theory was presented recently in [32] where the incremental plasticity theory for hardening was combined with an elastic fracturing theory for softening, thus bypassing the difficulties with non-positive definite tangential material with the aid of a total secant formulation. Different aspects of all these constitutive models for concrete were examined recently in [33].

#### 4. COMPUTATIONAL ASPECTS

On the structural level the total and differential forms of constitutive laws lead immediately to the well-known secant and tangential stiffness methods after appropriate discretisation with finite elements. The former approach determines directly the steady state equilibrium configuration by an iterative search technique while the latter traces the entire evolution path up to a certain state by tangential linearisation. The rate formulation involves thus the numerical integration of the entire process during which path-dependent effects are readily accounted for in contradistinction to the total equilibrium approach.

In the following, we examine different forms of incremental solution strategies for tracing the path of evolution of inelastic material processes. For illustration we will concentrate on elastic-viscoplastic material behaviour where the step by step integration is carried out in real time instead of a mechanically equivalent loading parameter which is used for rate-independent material problems.

The finite element method for elastic and inelastic material problems is well established. Therefore, we restrict ourselves to a brief summary of incremental equilibrium (principle of virtual power)

$$\int_V \delta \boldsymbol{\gamma}^t \Delta \boldsymbol{\sigma} \, dV = \int_V \delta \mathbf{u}^t \Delta \mathbf{p}_v \, dV + \int_S \delta \mathbf{u}^t \Delta \mathbf{p}_s \, dS \quad (4.1)$$

and the four classes of elastic-inelastic solution strategies which arise from different time integration methods of the constitutive rate equations [34], [35].

#### 4.1 Initial load methods

First we recall the traditional initial load strategies where the time operator is partitioned into an elastic and inelastic component. The elastic stiffness is used here as reference stiffness which is maintained constant during the entire evolution of the viscoplastic rate process

$$\dot{\boldsymbol{\eta}} = \mathbf{f}(\boldsymbol{\sigma}) = \frac{\mu}{3} \left( \frac{\bar{\boldsymbol{\sigma}}}{\bar{\boldsymbol{\sigma}}_y} - 1 \right) \boldsymbol{\sigma}_d \quad (4.2)$$

In the case of the direct forward approach the inelastic growth law is approximated by the explicit statement

$$\Delta \boldsymbol{\eta} = \Delta t \dot{\boldsymbol{\eta}} = \Delta t \mathbf{f}_0 \quad (4.3)$$

where  $\mathbf{f}_0$  indicates that only known state variables at the beginning of the time step are used  $\mathbf{f}_0 = \mathbf{f}(\boldsymbol{\sigma}_0)$ . The corresponding stress increment follows from the hypoelastic law

$$\Delta \boldsymbol{\sigma} = \mathbf{E}(\Delta \boldsymbol{\gamma} - \Delta t \mathbf{f}_0) \quad (4.4)$$

Substituting (4.4) into (4.1) yields the classical forward initial load method without iteration

$$\mathbf{K} \Delta \mathbf{r} = \Delta \mathbf{R} + \Delta \mathbf{J}_{\boldsymbol{\eta}}^0 \quad \text{with} \quad \Delta \mathbf{r} = \mathbf{r}_1 - \mathbf{r}_0 \quad (4.5)$$

where  $\mathbf{K}$  denotes the elastic stiffness matrix and  $\Delta \mathbf{J}_{\boldsymbol{\eta}}^0$  the initial loads due to the inelastic strain increment  $\Delta \boldsymbol{\eta} = \Delta t \mathbf{f}_0$ . The corresponding implicit formulation of the inelastic growth law involves yet unknown stresses within the time step  $\Delta t$  and thus requires iteration. The successive substitution method leads to a predictor-corrector scheme which updates the stress increment (4.4) according to the current values of the state variables, e.g. at the end of the time step if an overstable backward time operator is used

$$\Delta \boldsymbol{\sigma}^{i+1} = \mathbf{E}(\Delta \boldsymbol{\gamma}^i - \Delta t \mathbf{f}^i) \quad (4.6)$$



On the structural level we recover the iterative initial load method

$$\mathbf{K} \Delta \mathbf{r}^{\bar{i}+1} = \Delta \mathbf{R} + \Delta \mathbf{J} \eta^{\bar{i}} \quad (4.7)$$

in which the inelastic strain increment is corrected iteratively according to the current stress values within the time step  $\Delta t$ .

#### 4.2 Gradient methods

The application of the initial load methods is severely constrained by the time step restriction for stability and convergence [34], [35]. Although the resulting time marching strategy assures a very accurate viscoplastic solution it is rather expensive when the entire transient response history has to be integrated. The tangential stiffness methods are able to overrule these time step restrictions and thus provide more flexibility although at the cost of more elaborate computations.

In the case of the forward gradient approach the stress increment is defined by

$$\Delta \boldsymbol{\sigma} = \mathbf{E}_{\tau}^{\circ} (\Delta \boldsymbol{\gamma} - \Delta t \dot{\boldsymbol{f}}_o) \quad \text{where} \quad \mathbf{E}_{\tau}^{\circ} = \left( \mathbf{E}^{-1} + \Delta t \frac{\partial \dot{\boldsymbol{f}}_o}{\partial \boldsymbol{\sigma}} \right)^{-1} \quad (4.8)$$

In the forward strategy the tangential material law  $\mathbf{E}_{\tau}^{\circ}$  and the inelastic growth law  $\dot{\boldsymbol{f}}_o$  are both evaluated at the beginning of the time step. Therefore no iteration is required and the computation on the structural level corresponds to the simplest form of the incremental tangential stiffness method without iterative correction

$$\mathbf{K}_{\tau}^{\circ} \Delta \mathbf{r} = \Delta \mathbf{R} + \Delta \mathbf{J} \eta^{\circ} \quad (4.9)$$

In this method the time steps are limited by accuracy rather than stability. Moreover, the viscoplastic overstress model introduces elastic unloading effects when too large time steps are used. In this case, when the long-term steady state conditions are of prime concern, the backward gradient approach must be used in spite of the computational complexities with the resulting Newton-Raphson scheme.

In the Newton-Raphson technique the residual  $\delta^i$  of the incremental constitutive relations is reduced to zero

$$\delta^{\bar{i}} = \Delta \boldsymbol{\gamma}^{\bar{i}} - \Delta t \dot{\boldsymbol{f}}^{\bar{i}} - \mathbf{E}^{-1} \Delta \boldsymbol{\sigma}^{\bar{i}} \quad \text{and} \quad \delta^{\bar{i}+1} = \delta^{\bar{i}} + d \delta^{\bar{i}} = 0 \quad (4.10)$$

The resulting stress corrections at the end of the time step are then

$$d \boldsymbol{\sigma}^{\bar{i}} = \mathbf{E}_{\tau}^{\bar{i}} (d \boldsymbol{\gamma}^{\bar{i}} - \delta^{\bar{i}}) \quad (4.11)$$

where the tangential material law is evaluated at the end of the time step

$$\mathbf{E}_{\tau}^{\bar{i}} = \left( \mathbf{E}^{-1} + \Delta t \frac{\partial \dot{\boldsymbol{f}}^{\bar{i}}}{\partial \boldsymbol{\sigma}} \right)^{-1} \quad (4.12)$$



On the structural level the unbalanced load due to the change of internal stresses  $d\mathbf{\sigma}^j$  is at the end of the time step

$$\int_V \delta \boldsymbol{\gamma}^t d\mathbf{\sigma}^j dV = \mathbf{R}_j - \int_V \delta \boldsymbol{\gamma}^t \mathbf{\sigma}_i^j dV \quad (4.13)$$

Substituting (4.11) into the incremental equilibrium condition (4.13) yields the tangential relation for the displacement correction  $d\mathbf{r}^j$

$$\mathbf{K}_T^j d\mathbf{r}^j = \mathbf{F}^j \quad (4.14)$$

$\mathbf{K}_T^j$  denotes here the tangential structural stiffness corresponding to  $\mathbf{E}_T^j$  in (4.12) and  $\mathbf{F}^j$  the unbalanced load due to the constitutive error  $\delta^j$  (4.10)

$$\mathbf{F}^j = \mathbf{R}_j + \int_V \delta \boldsymbol{\gamma}^t (\mathbf{E}_T^j (-\Delta \boldsymbol{\gamma}^j + \Delta t \dot{\mathbf{f}}^j + \mathbf{E}^{-1} \Delta \mathbf{\sigma}^j) - \mathbf{\sigma}_i^j) dV \quad (4.15)$$

As indicated before, the straight Newton-Raphson algorithm calls for formation and factorisation of the structural gradient matrix  $\mathbf{E}_T^j$  at each cycle of iteration. The computational effort can be reduced by updating the tangential stiffness only occasionally, e.g. at the beginning of a new time step (modified Newton-Raphson technique). In the limit we maintain the elastic stiffness as structural gradient matrix during the entire viscoplastic process and recover the iterative initial load method above. However, the convergence limitations of this approach ask for alternative computational strategies such as the quasi-Newton methods. The most promising candidate is the BFGS-algorithm of Broyden-Fletcher-Goldfarb and Shanno which was developed originally in the context of optimisation and which was subsequently applied to different finite element problems [35], [36], [37].

### 4.3 BFGS-method

The quasi-Newton method is essentially a search technique for the new solution  $\mathbf{r}_{k+1}$  according to

$$\mathbf{r}_{k+1} = \mathbf{r}_k + s_k \mathbf{d}_k \quad (4.16)$$

using the secant relation

$$\left. \begin{array}{l} \mathbf{K}_k \mathbf{d}_k = \mathbf{r}_k \\ \text{where } \mathbf{d}_k = \mathbf{r}_k - \mathbf{r}_{k-1} \\ \text{and } \mathbf{r}_k = \mathbf{F}_k - \mathbf{F}_{k-1} \end{array} \right\} \quad (4.17)$$

The vector  $\mathbf{d}_k$  denotes the search direction and  $s_k$  the scalar which satisfies the orthogonality condition

$$\mathbf{d}_k^t \mathbf{F}_{k+1} = 0 \quad (4.18)$$



The BFGS-method is based on a series of rank two modifications which can be directly applied in order to update the inverse  $\mathbf{K}^{-1}$

$$\mathbf{K}_{k}^{-1} = (\mathbf{I} + \omega_k \mathbf{v}_k \mathbf{v}_k^t) \mathbf{K}_{k-1}^{-1} (\mathbf{I} + \mathbf{v}_k \omega_k^t) \quad (4.19)$$

where the new search direction follows from

$$\mathbf{d}_k = \mathbf{K}_{k-1}^{-1} \mathbf{F}_k \quad (4.20)$$

The scalar  $s_k$  is obtained by line search for zero  $\mathbf{F}_k$  along  $\mathbf{d}_k$  if the orthogonality condition (4.18) exceeds an assumed threshold. The modification vectors  $\mathbf{v}_k$  and  $\omega_k$  are defined as

$$\mathbf{v}_k = \mathbf{F}_{k-1} \left( 1 + s_{k-1} \left( \frac{\mathbf{d}_{k-1}^t \mathbf{F}_k}{\mathbf{d}_{k-1}^t \mathbf{F}_{k-1}} \right)^2 \right) - \mathbf{F}_k \quad (4.21)$$

$$\omega_k = \frac{1}{\mathbf{d}_k^t \mathbf{F}_k} \delta_k \quad (4.22)$$

Note the index  $k$  is used here in order to distinguish the BFGS-iteration from the Newton step (4.14) and the predictor-corrector method (4.7). Clearly, a sufficiently large number of BFGS-modifications correspond to a single Newton step, thus asymptotically we maintain the same range of convergence and circumvent the tight time step restrictions of the iterative initial load method. On the computational side the BFGS-method involves repeated modification of the triangular factor. The recursion formula (4.19) indicates that each iteration cycle involves a series of vector operations on the right-hand side. Clearly, for an efficient solution the number of iterations must be limited to a small number since the computational effort grows rapidly with each additional iteration. Normally, 3 - 7 iterations were sufficient to attain satisfactory convergence for large time step viscoplastic solutions where the elastic stiffness is retained as reference stiffness.

COMPUTATIONAL METHOD	DIRECT FORWARD $\zeta = 0$	ITERATIV CORRECTION $\zeta > 0$
INITIAL LOAD $\mathbf{E} \rightarrow \mathbf{K}$	DIM $\Delta t < \Delta t_s$ $\mathbf{K} \Delta \mathbf{r} = \Delta \mathbf{R} \cdot \Delta \mathbf{J}_\eta^0$	NIM $\Delta t < \Delta t_c$ $\mathbf{K} \Delta \mathbf{r}^i = \Delta \mathbf{R} \cdot \Delta \mathbf{J}_\eta^i$
TANG. STIFFNESS $\mathbf{E}_T \rightarrow \mathbf{K}_T$	DTS $\mathbf{K}_T^0 \Delta \mathbf{r} = \Delta \mathbf{R} \cdot \Delta \mathbf{J}_\eta^0$	N-R $\mathbf{K}_T^j \Delta \mathbf{r}^j = \mathbf{F}_\zeta^j$ BFGS: $\mathbf{a}_{k+1} = \mathbf{a}_k + s_k \mathbf{d}_k$

Table 1: COMPUTATIONAL STRATEGIES FOR VISCOPLASTIC ANALYSIS

The four computational strategies are summarised in Table 1. The BFGS-method belongs to the class of iterative gradient methods, although the viscoplastic implementation operates with a constant elastic reference stiffness analogous to the iterative initial load method. The initial load methods exhibit stringent stability and convergence limits  $\Delta t_s, \Delta t_c$  which severely restrict the time steps [34]. It is intriguing that for rate independent plasticity no such convergence limit exists if the NIM-method is implemented within the initial stress formulation [38].

#### 4.4 Viscoplastic solution of pressurised cylinder

For illustration we consider a thick-walled cylinder which is subjected to increasing internal pressure. Both the nonlinear response behaviour and the limit load behaviour are of interest when a viscoplastic overstress model is used to predict the transient phase up to steady state conditions. For simplicity a nonhardening viscoplastic model using (4.2) is used with  $\bar{\sigma}_y = \text{const.}$  in order to compare the steady state solution with that of the elastic - ideally plastic solution of Prager and Hodge [39].

Fig. 8 shows the basic lay-out and the idealisation with axisymmetric finite elements. The particular material properties are taken from a previous study [40] and are typical for a mild steel with

$$\begin{aligned}
 E &= 30 \times 10^6 \text{ psi} \quad , \quad \nu = 0.30 \\
 \bar{\sigma}_y &= 30 \times 10^3 \text{ psi} \quad , \quad \mu = 10^{-8} \text{ sec/psi}
 \end{aligned}
 \tag{4.23}$$

Fig. 9 shows the load-displacement relationship under increasing pressure. The solid line indicates the steady state elastic - ideally plastic solution which bounds the nonlinear response between the elastic limit  $p_e = 12968 \text{ psi}$  and the plastic limit pressure  $p_p = 24011 \text{ psi}$ . In the viscoplastic analysis various pressure levels ( $p_i = 13, 18, 21, 24$  and  $25 \times 10^3 \text{ psi}$ ) were applied directly without incrementation, and the ensuing viscoplastic response was traced starting from the initial elastic overstress condition up to the steady state solution which approaches asymptotically the elastic-plastic response at  $t \rightarrow \infty$ . Even for an internal pressure of  $p_i = 24000 \text{ psi}$  a stable steady state solution was reached while for  $p_i = 25000 \text{ psi}$  the remaining overstress resulted in continuous outward flow.

The intrinsic performance of the previous computational strategies is illustrated with the equivalent stress history at the inside wall. Fig. 10 compares the prediction of the BFGS-algorithm with that of the direct forward methods with and without tangential stiffness. In the case of the DIM forward initial load scheme the constant time steps  $\Delta t = 1 \text{ sec}$  lead to elastic unloading because of the critical time step for stability  $\Delta t_s = 1.3 \text{ sec}$ . In contrast the implicit BFGS algorithm provides high accuracy and exhibits far less numerical damping than the DTS forward gradient strategy. Note that the elastic stiffness matrix was retained in the BFGS and the DIM algorithms during the entire viscoplastic process while satisfactory convergence was obtained with the BFGS quasi-Newton method within 2 - 3 iterations.

Finally, the rapid deterioration of the forward gradient solution is shown in Fig. 11 where the equivalent stress distribution across the cylinder wall is plotted for a larger time step of  $\Delta t = 10$ . In this case, only the backward time operator is suitable for predicting the steady state condition within a single time step since the initial elastic overstresses relax to zero and lead to oscillations if they are included in the forward and midstep algorithms. As a



matter of fact, the forward gradient method utilises only the initial elastic information at the beginning of the time step for the evaluation of the tangential stiffness matrix. This aspect leads to forward gradient predictions which are completely erroneous for large time steps such as  $\Delta t = 1000$ , while the BFGS-algorithm yields still satisfactory results of the steady state elastic plastic solution within 13 iterations.

In conclusion, the BFGS-quasi-Newton method is very flexible - it provides very accurate solutions in the transient response regime and it readily accomodates very large time steps when the limiting steady state plastic solution is of primary concern. The viscoplastic solution is obtained with an elastic stiffness matrix which remains constant during the entire time history analysis. Therefore the BFGS-algorithm corresponds formally to the traditional initial load methods where the entire inelastic process is converted into equivalent driving forces on the right-hand side.

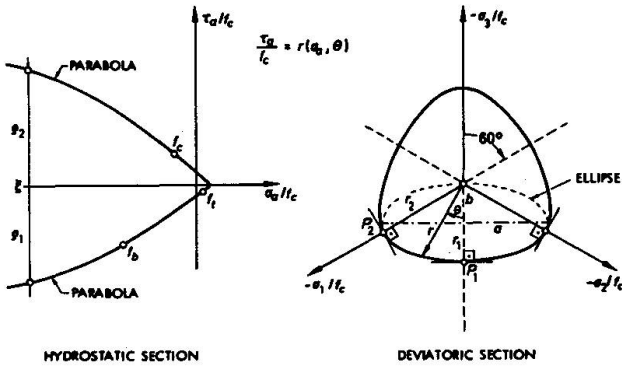


Fig. 1 CONSTRUCTION OF FIVE PARAMETER MODEL

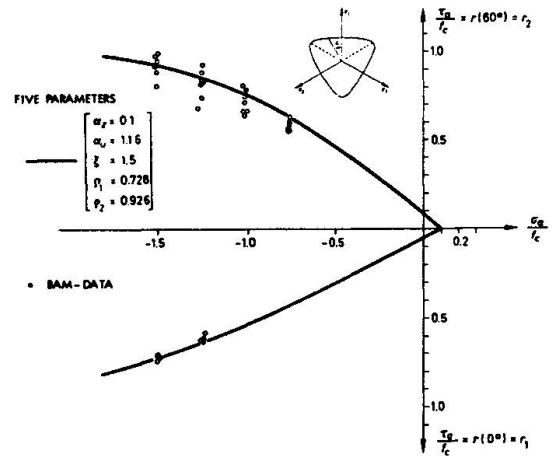


Fig. 2 FIVE PARAMETER MODEL, HYDROSTATIC SECTION

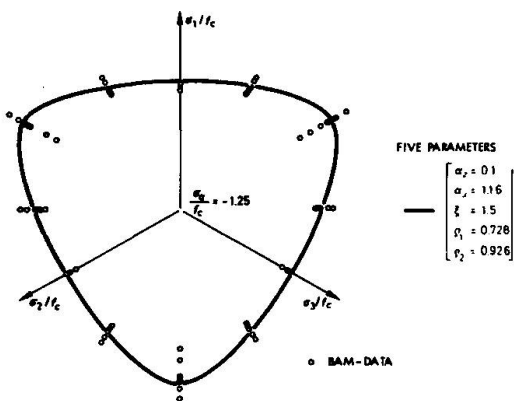


Fig. 3 FIVE PARAMETER MODEL, DEVIATORIC SECTION

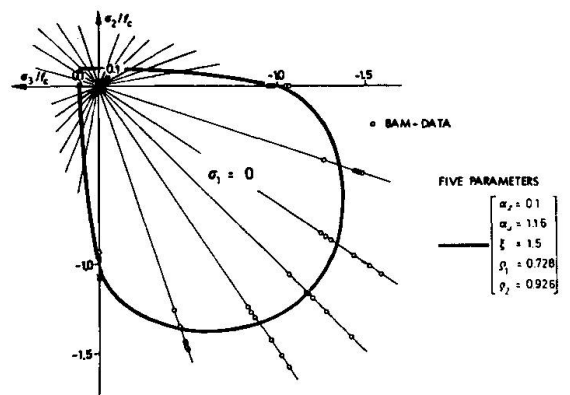


Fig. 4 FIVE PARAMETER MODEL, BIAxIAL SECTION

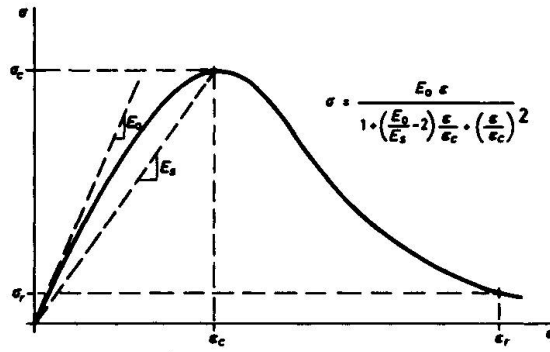


Fig. 5 UNIAXIAL COMPRESSION MODEL

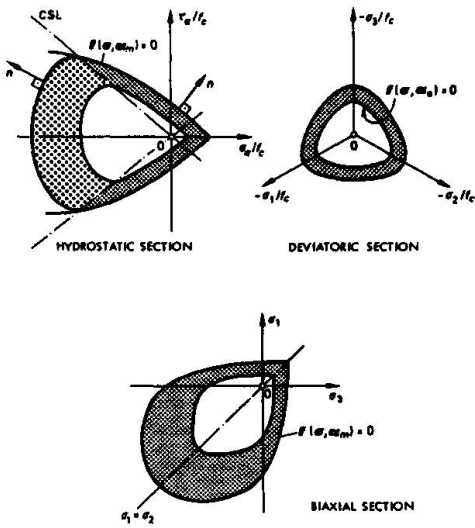


Fig. 6 HARDENING FIVE-PARAMETER MODEL

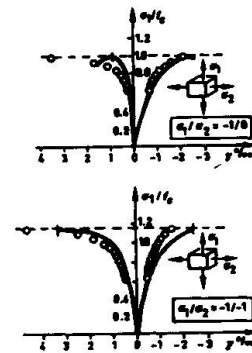


Fig. 7 COMPARISON WITH BIAXIAL TEST DATA [KUPFER et al.]

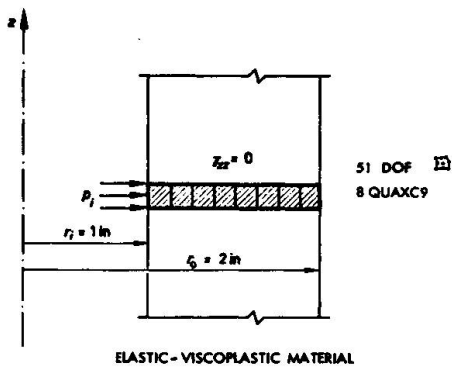


Fig. 8: THICK-WALLED CYLINDER UNDER INTERNAL PRESSURE

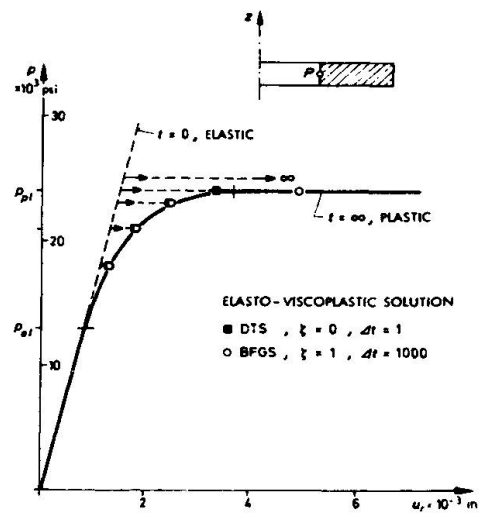


Fig. 9: LOAD - DISPLACEMENT BEHAVIOUR

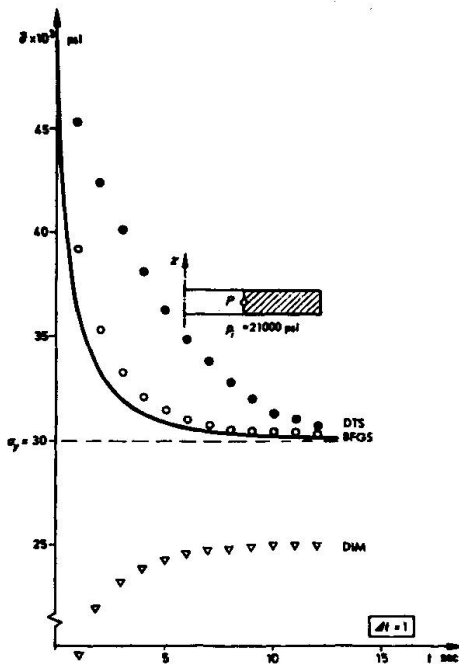
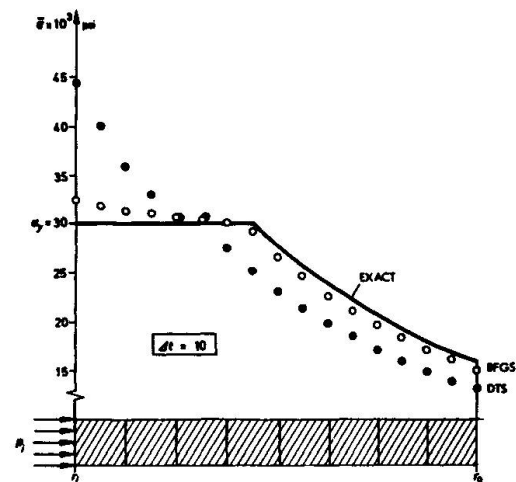


Fig. 10: EQUIVALENT STRESS HISTORY AT THE INSIDE WALL

Fig. 11: EQUIVALENT STRESS DISTRIBUTION AT THE TIME  $t = 10$  sec

## REFERENCES

- [1] A.C. SCORDELIS, Finite Element Analysis of Reinforced Concrete Structures, The Finite Element Method in Civil Engng. (McGill Univ. Montreal 1972)
- [2] J.H. ARGYRIS, G. FAUST, J. SZIMMAT, E.P. WARNKE, K.J. WILLAM, Recent Developments in the Finite Element Analysis of Prestressed Concrete Reactor Vessels, Nucl. Eng. Design. 28 (1974) 42-75
- [3] W.C. SCHNOBRICH, Behaviour of Reinforced Concrete Structures Predicted by the Finite Element Method, Comp. Struct. 7 (1977) 365-376
- [4] P.G. BERGAN, I. HOLLAND, Nonlinear Finite Element Analysis of Concrete Structures, Comp. Meths. Appl. Mech. Eng. 17/18 (1979) 443-467
- [5] K.H. GERSTLE, D.H. LINSE et al., Strength of Concrete under Multiaxial Stress States, Proc. McHenry Symp., ACI SP55, Mexico City, 1976
- [6] D.H. LINSE, H. ASCHL, Versuche zum Verhalten von Beton unter mehrachsiger Beanspruchung, Internal Report of Concrete Institute, Technical University Munich (1976)
- [7] G. SCHICKERT, H. WINKLER, Versuchsergebnisse zur Festigkeit und Verformung von Beton bei mehraxialer Druckbeanspruchung, DAfStb Heft 277, 1977
- [8] B. PAUL, Macroscopic Criteria for Plastic Flow and Brittle Fracture, in Fracture, an Advanced Treatise, H. Liebowitz ed., Academic Press (1968) 313-491
- [9] J.H. ARGYRIS, G. FAUST, K.J. WILLAM, Limit Load Analysis of Thick-Walled Concrete Structures - A Finite Element Approach to Fracture, Comp. Meths. Appl. Mech. Eng. 8 (1976) 215-243
- [10] K.J. WILLAM, E.P. WARNKE, Constitutive Model for the Triaxial Behaviour of Concrete, ISMES Seminar on Concrete Structures Subjected to Triaxial Stresses, Bergamo, May 17-19, 1974, Proc. IABSE Report No. 19, Zurich, 1975

- [11] N.S. OTTOSEN, A Failure Criterion for Concrete, *J. ASCE EM4* (1977) 527-535
- [12] J. WASTIELS, Failure Criteria for Concrete under Multiaxial Stress States, *Proc. IABSE Coll. on Plasticity in Reinforced Concrete, Copenhagen, May 21-23, 1979*
- [13] I. NELSON, M.L. BARON, I.S. SANDLER, *Mathematical Models for Geological Materials for Wave Propagation Studies, Shock Waves and the Mechanical Properties of Solids, Syracuse University Press, Syracuse, N.Y. (1971)*
- [14] D.W. MURRAY, Octahedral Based Incremental Stiffness Matrices, *ASCE, 105, EM4* (1979) 501-514
- [15] T.C.Y. LIU, A.H. NILSON, F.O. SLATE, Biaxial Stress-Strain Relations for Concrete, *ASCE 98, ST5* (1972) 1025-1034
- [16] J. LINK, Eine Formulierung des zweiaxialen Verformungs- und Bruchverhaltens von Beton, *Deutscher Ausschuß für Stahlbeton, Heft 270, Berlin 1976*
- [17] D. DARWIN, D.A. PECKNOLD, Nonlinear Biaxial Stress-Strain Law for Concrete, *ASCE EM2* (1977) 229-241
- [18] A.A. ELWI, D.W. MURRAY, A 3 D Hypoelastic Concrete Constitutive Relationship, *ASCE 105, EM4* (1979) 623-641
- [19] N.S. OTTOSEN, Constitutive Model for Short-Term Loading of Concrete, *ASCE 105, EM1* (1979) 127-141
- [20] M.D. COON, R.J. EVANS, Incremental Constitutive Laws and their Associated Failure Criteria with Application to Plain Concrete, *Int. J. Solids Struct. 8* (1972) 1169-1180
- [21] H. KAUDERER, Über ein nichtlineares Elastizitätsgesetz, *Ing. Archiv 17* (1949) 450-480
- [22] H.B. KUPFER, K.H. GERSTLE, Behaviour of Concrete under Biaxial Stresses, *ASCE 99, EM4* (1973) 853-866
- [23] K.H. GERSTLE, H. ASCHL et al., Behaviour of Concrete under Multiaxial Stress States, to appear in *ASCE ST* (1980)
- [24] M.D. KOTSOVOS, J.B. NEWMAN, A Model of Concrete Behaviour under Generalised Stress, *Proc. IABSE Coll. on Plasticity in Reinforced Concrete, Copenhagen, May 21-23, 1979*
- [25] B.P. SINHA, K.H. GERSTLE, L.G. TULIN, Stress-Strain Relations for Concrete under Cyclic Loading, *ACI J. 61* (1964) 195-210
- [26] A.C.T. CHEN, W.-F. CHEN, Constitutive Relations for Concrete, *ASCE 101, EM4* (1975) 465-481
- [27] J.H. ARGYRIS, G. FAUST, K.J. WILLAM, A Unified Stress-Strain Law for Triaxial Concrete Failure, *3rd Post Conf. on Comput. Aspects of the FEM, Imperial College, London, Sept. 8-9 (1975), G. Davies ed., London, 1975, 359-402*
- [28] D.W. MURRAY, L. CHITNUYANONDH, K.Y. RIJUB-AGHA, CHUNG WONG, A Concrete Plasticity Theory for Biaxial Stress Analysis, *ASCE 105, EM6* (1979) 989-1006
- [29] Z.P. BAZANT, P. BHAT, Endochronic Theory of Inelasticity and Failure of Concrete, *ASCE 102, EM4* (1976) 701-722



- [30] Z.P. BAZANT, Endochronic Inelasticity and Incremental Plasticity, *Int. J. Solids Struct.* 14 (1978) 691-714
- [31] I.S. SANDLER, On the Uniqueness and Stability of Endochronic Theories of Material Behaviour, *J. Appl. Mech.* 45 (1978) 263-266
- [32] Z.P. BAZANT, S.-S. KIM, Plastic-Fracturing Theory of Concrete, *ASCE* 105, EM3 (1979) 407-428
- [33] W.F. CHEN, E.C. TING, Constitutive Models for Concrete Structures, *ASCE* 106, EM1 (1980) 1-20
- [34] J.H. ARGYRIS, L.E. VAZ, K.J. WILLAM, Improved Solution Methods for Inelastic Rate Problems, *Comp. Meths. Appl. Mech. Eng.* 16 (1978) 231-277
- [35] J.H. ARGYRIS, L.E. VAZ, K.J. WILLAM, Integrated Finite Element Analysis of Coupled Thermoviscoplastic Problems, *ISD Report No. 283*, University of Stuttgart (1980)
- [36] H. MATTIES, G. STRANG, The Solution of Nonlinear Finite Element Equations, *Int. J. Num. Meth. Eng.* 11 (1979) 1613-1626
- [37] K.-J. BATHE, A.P. CIMENTO, Some Practical Procedures for the Solution of Non-linear Finite Element Equations, *Comp. Meths. Appl. Mech. Eng.* 22 (1980) 59-85
- [38] J.H. ARGYRIS, D.W. SCHARPF, Methods of Elasto-Plastic Analysis, *Proceed. ISA-ISSC Symp., Stuttgart 1969*, 381-416, *ZAMP* 23 (1972) 517-551
- [39] W. PRAGER, Ph. G. HODGE Jr., *Theory of Perfectly Plastic Solids*, J. Wiley, New York 1951
- [40] T.J.R. HUGHES, R.L. TAYLOR, Unconditionally Stable Algorithms for Quasistatic Elasto/Visco-Plastic Finite Element Analysis, *Computer & Struct.* 8 (1978) 169-173